VU VRIJE UNIVERSITEIT AMSTERDAM

# VU Research Portal

## Resonance CARS in BrZ

Intense, C.

***published in***
Chemical Physics Letters
1992

***document version***
Publisher's PDF, also known as Version of record

**Link to publication in VU Research Portal**

***citation for published version (APA)***
Intense, C. (1992). Resonance CARS in BrZ. *Chemical Physics Letters*.

**General rights**
Copyright and moral rights for the publications made accessible in the public portal are retained by the authors and/or other copyright owners and it is a condition of accessing publications that users recognise and abide by the legal requirements associated with these rights.

- Users may download and print one copy of any publication from the public portal for the purpose of private study or research.
- You may not further distribute the material or use it for any profit-making activity or commercial gain
- You may freely distribute the URL identifying the publication in the public portal

**Take down policy**
If you believe that this document breaches copyright please contact us providing details, and we will remove access to the work immediately and investigate your claim.

**E-mail address:**
**vuresearchportal.ub@vu.nl**

Download date: 03. Aug. 2024

# Resonance CARS in $Br_2$

Ilse Aben, Wim Ubachs, Gert van der Zwan and Wim Hogervorst
*Laser Centre, Free University Amsterdam, De Boelelaan 1081, 1081 HV Amsterdam, The Netherlands*

Received 7 July 1992

Intense CARS spectra were observed in bromine vapour, which could be attributed to resonances in the molecular as well as atomic species. From accurate measurements of frequency positions and polarization dependencies a vibrational overtone sequence $\Delta v = 2$–12, characteristic for resonance CARS, was identified for $Br_2$. Doublets of rotational lines reveal enhancement by discrete transitions between bound states in the molecular medium.

## 1. Introduction

Since the first observation of resonance Raman scattering in gases by Holzer et al. [1] over two decades ago, many experimental and theoretical efforts have been undertaken to explain the spectral and dynamical phenomena observed. The work concentrated on the simple diatomic molecules $I_2$ and $Br_2$ with a single vibrational mode and excited electronic states that are easily accessible with visible lasers. Furthermore, molecular iodine and bromine are well studied systems and their molecular constants are known to a high level of accuracy.

The difference between conventional off-resonance Raman, discrete resonance Raman and continuum resonance Raman processes in terms of spectral distributions and dynamical response time was explained by Rousseau and Williams [2,3]. A dominant spectral feature in resonance Raman scattering is the appearance of intense overtones, which are orders of magnitude weaker in conventional off-resonance Raman. In discrete resonance Raman processes overtones are also observed but then only rotational doublets are seen, opposed to the process of continuum resonance Raman showing complete rotational branches. Continuum resonance Raman processes were observed in $Br_2$ by Kiefer and Baierl [4]. Various groups have worked successfully on a theoretical description of the effects in continuum resonance Raman spectra in terms of Franck–Condon overlap integrals [3,5,6]. The contribution of continua of different states and of interferences, e.g. the combined effect of the $^1\Pi_{1u}$ and $B\,^3\Pi^+_{u0}$ continua in resonance Raman spectra of $I_2$ and $Br_2$, is also described.

A coherent form of continuum resonance Raman scattering (CARS) was observed by Beckmann et al. [7] in molecular iodine. Recently several multiple resonance four-wave-mixing processes in $I_2$ were identified. Enhancement by discrete states at the one-photon level and by a dissociative continuum state at the two-photon level was analyzed [8]; moreover new excited-state CARS processes were identified.

In this paper, we report on the observation of resonance-enhanced CARS in natural bromine in a two-colour experiment. Apart from the Raman-resonance on a vibrational excitation ($\Delta\omega = \omega_1 - \omega_2$) the coherent four-wave-mixing process is enhanced on the pump wave ($\omega_1$) by an electronic resonance, a discrete rotational transition in the $B\,^3\Pi^+_{u0}$–$X\,^1\Sigma^+_g$ system, as well as on the anti-Stokes wave ($\omega_{AS} = 2\omega_1 - \omega_2$) by another electronic resonance. The latter resonance is the combined effect of the dissociative continuum of the bound $B\,^3\Pi^+_{u0}$ state and the repulsive $^1\Pi_{1u}$ state. As in the experiments on doubly-enhanced continuum CARS [7] a long progression of overtones ($\Delta v = 2$–12) is observed. However, in the present form of the discrete resonance CARS

*Correspondence to:* W. Ubachs, Laser Centre, Free University Amsterdam, De Boelelaan 1081, 1081 HV Amsterdam, The Netherlands.

0009-2614/92/$ 05.00 © 1992 Elsevier Science Publishers B.V. All rights reserved.

extremely narrow features, related to single rotational lines, are observed. On the basis of frequency positions and depolarization ratios the four-wave sequence of the CARS process can be identified with appropriate quantum numbers for the enhancing states involved. Rotational linestrengths are compared with theoretically derived values and agreement is found. Also the contributions of molecular isotopes ($^{79}Br^{79}Br$, $^{79}Br^{81}Br$, or $^{81}Br^{81}Br$) to a singly resolved narrow feature may be readily identified. In this sense the discrete resonance CARS excitations are isotope selective.

## 2. Experimental

A standard colinear CARS setup was used with an injection-seeded frequency-doubled Nd:YAG laser at 532 nm as the pump laser ($\omega_1$), and a pulsed dye-laser with a bandwidth of 0.07 $cm^{-1}$ for the tunable Stokes beam ($\omega_2$). A spectral region of 600–3800 $cm^{-1}$ for the Raman shift $\omega_1-\omega_2$ was covered using different dyes. Accurate calibration of the Stokes frequency (within 0.015 $cm^{-1}$) was performed by interpolation between lines of a simultaneously recorded fluorescence spectrum of $I_2$. The two beams in the CARS setup were spatially overlapped with a dichroic mirror and focused with a $f=25$ cm lens in a cell containing about 3 Torr natural bromine (50.69% $^{79}Br$ and 49.31% $^{81}Br$, so $^{79,79}Br_2$: $^{79,81}Br_2$: $^{81,81}Br_2 \approx 1:2:1$). The CARS signal at $\omega_{AS}=2\omega_1-\omega_2$ was separated from the fundamental beams $\omega_1$ and $\omega_2$ using a bandpass filter and a three-stage monochromator and detected with a photomultiplier. Spectra were obtained by averaging over several laser shots per frequency setting. In all experiments the beams were linearly polarized and in most cases parallel polarization of the two beams was used. In the crossed polarization experiment a $\frac{1}{2}\lambda$ plate was used to rotate the polarization of the $\omega_1$ beam.

A note should be made here on the spectral characteristics of the injection-seeded version of the frequency-doubled Nd:YAG laser (Quanta Ray GCR-3) as far as they are crucial for the present experiment. When properly seeded the pulsed Nd:YAG laser runs on a single longitudinal cavity mode and its bandwidth is close to the Fourier transform limit, so $\delta\omega<0.005$ $cm^{-1}$. The cavity length of the pulsed laser is actively stabilized to remain in resonance with a cw miser seed-laser. The cw seed laser operates within the gain profile of Nd:YAG, $\approx 1$ $cm^{-1}$ wide. The exact frequency of the pulsed Nd:YAG laser is determined by the temperature control setting of the miser seed-lasing system, that may be subject to day-to-day variations within the gain profile. Accurate measurement of the frequency of a non-scanning pulsed laser is in general a problem, and we relied on an echelle-grating monochromator with a limited accuracy. The pump frequency of the frequency-doubled Nd:YAG laser was thus determined at $18788.5\pm0.2$ $cm^{-1}$. The piezo voltage in the feedback-loop regulating the length of the pulsed laser cavity, can be used to verify that during the experiment no mode-hops occur in the single-longitudinal mode output of the pulsed laser. In the absence of mode-hops the frequency $\omega_1$ is constant within 0.01 $cm^{-1}$. In section 3 we will discuss a method for a more accurate frequency calibration of the Nd:YAG laser from the observed CARS spectra.

## 3. Measurements and interpretation

### *3.1. Resonance CARS in molecular bromine: frequency positions*

A sequence of repeating groups of spectral lines was recorded in a wide frequency range for a Raman shift $\omega_1-\omega_2=600$–$3800$ $cm^{-1}$. This sequence was identified as a series of overtones $\Delta v=2$–$12$ in the electronic ground state $X\,^1\Sigma_g^+$ of $Br_2$. As an example in fig. 1 the most intense part of the resonance-enhanced CARS spectrum of $\Delta v=7$ in $Br_2$ is shown. The spectrum consists of an irregular pattern of narrow resonances reflecting the width of the dye laser. In the lower part of fig. 1a simultaneously recorded $I_2$-fluorescence spectrum is shown that determines the frequency calibration of the Stokes laser. The accuracy in the interpolated positions of the CARS resonances is 0.015 $cm^{-1}$ on the $\omega_2$ scale. The sequence of overtones is observed as a repeating spectral fingerprint with a spacing of about 300 $cm^{-1}$. CARS spectra of two adjacent overtones $\Delta v=7$ and $\Delta v=8$ are shown in fig. 2, where corresponding rotational transitions in both spectra are interconnected by

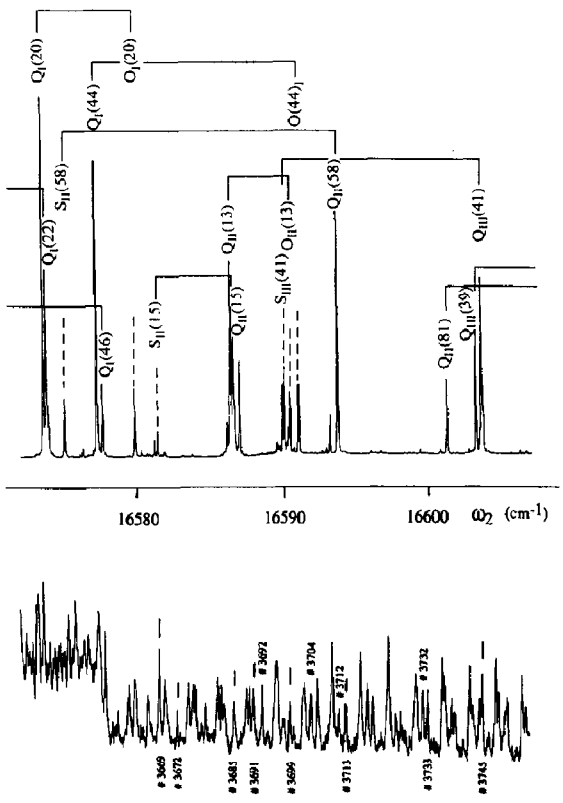


Fig. 1. Part of the resonance-enhanced CARS spectrum of $\Delta v=7$ in $Br_2$. The different isotopes are denoted by the subscripts I($^{79,79}Br_2$), II($^{79,81}Br_2$) and III($^{81,81}Br_2$). The Raman resonances in the electronic ground state are denoted by O, Q and S and with the $J$ value of the initial rotational state (in between brackets). The frequency scale is derived from the $I_2$-fluorescence spectrum recorded simultaneously (shown in lower part). The lines used for the interpolation and extrapolation of the frequency scale are marked with # and a number corresponding to the $I_2$ atlas [10].

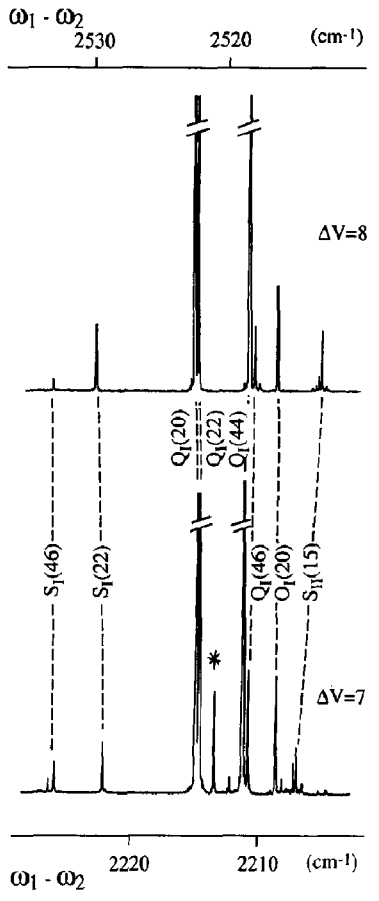


Fig. 2. Corresponding Raman resonances of adjacent overtones in the $\Delta v=7$ (lower spectrum) and $\Delta v=8$ (upper spectrum) CARS spectra. The line denoted by the asterisk is the $S_{II}(58)$.

dashed lines. The small relative frequency shifts between related resonances reflect the vibrational dependence of the rotational constants. Fig. 3 shows polarization effects in the resonance CARS linestrengths, again for the $\Delta v=7$ overtone. A spectrum recorded with parallel polarizations of the two incoming laser beams at frequencies $\omega_1$ and $\omega_2$ is compared to a spectrum taken with crossed polarizations; both beams were linearly polarized during these measurements. The strong relative intensity changes indicate that the spectra are strongly polarization dependent.

For an interpretation and assignment of the observed CARS features in figs. 1–3 we will start with an inspection of the third-order nonlinear susceptibility $\chi^{(3)}(\omega_{AS})$ that governs the intensity of the resonances through

$$I_{CARS} \propto |\chi^{(3)}_{CARS}|^2 I^2(\omega_1) I(\omega_2)\,. \qquad (1)$$

In general in four-wave mixing (FWM) this nonlinear susceptibility $\chi^{(3)}$ consists of 48 different terms. Because of the double degeneracy on the pump frequency $\omega_1$ only 24 terms remain for CARS. Assuming the specific energy level scheme for bromine as depicted in fig. 4a, with a bound electronic ground state $X\,^1\Sigma_g^+$ and a bound excited electronic state $B\,^3\Pi_{u0}^+$ at the one-photon level, only one of the 24 terms exhibits threefold enhancement on a discrete electronic resonance, on a discrete Raman resonance in the ground state and on an anti-Stokes continuum

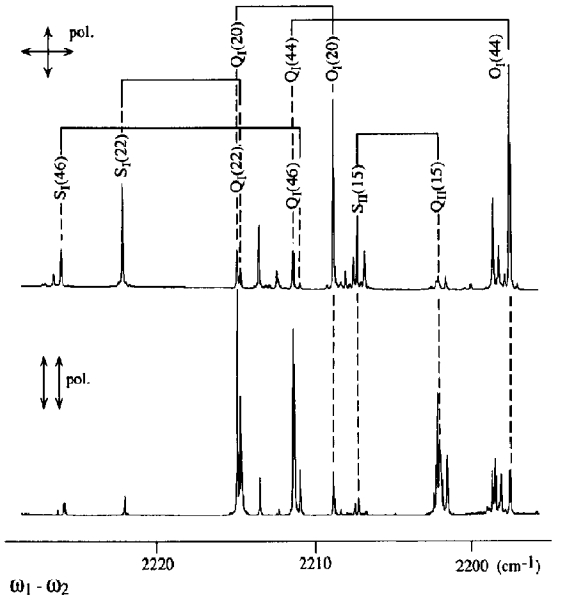


Fig. 3. Polarization effects in the $\Delta v = 7$ resonance-enhanced CARS spectrum. Upper spectrum: crossed polarizations of beams with frequencies $\omega_1$ and $\omega_2$. Lower spectrum: parallel polarizations. Both polarizations are linear.

resonance simultaneously [8]. This is only true under the condition that the generated anti-Stokes frequency $\omega_{AS} = 2\omega_1 - \omega_2$ reaches into the continuum above the dissociation limit of the $B\,^3\Pi^+_{u0}$ state: $D_0(B) = 19579.692$ ($^{79,79}Br_2$), 19580.695 ($^{79,81}Br_2$) and 19581.706 ($^{81,81}Br_2$) [9], which is realized in our experiments. Thus, the only remaining term of $\chi^{(3)}$ involving a doubly discrete resonance and a continuum resonance (illustrated in the generalized energy level scheme of fig. 4b) is given by [8]

$$\chi^{(3)}_{\rho\sigma\tau\nu}(\omega_{AS};\omega_1,\omega_1,-\omega_2) \propto N \sum_{a,b,c,d} \rho^{(0)}_{aa} \times \langle a|\mu_\sigma|b\rangle\langle b|\mu_\nu|c\rangle\langle c|\mu_\tau|d\rangle\langle d|\mu_\rho|a\rangle \times [(\omega_{ba} - \omega_1 - i\Gamma_{ba})(\omega_{ca} - \omega_1 + \omega_2 - i\Gamma_{ca}) \times (\omega_{da} - \omega_{AS} - i\Gamma_{da})]^{-1}. \quad (2)$$

The states $|a\rangle$, $|b\rangle$, $|c\rangle$ and $|d\rangle$ are labelled according to the energy scheme of fig. 4. The sum is over bound states $|a\rangle$, $|b\rangle$ and $|c\rangle$ and continuum states $|d\rangle$. The number density of $Br_2$ molecules is denoted by $N$ and $\rho^{(0)}_{aa}$ is the initial population of state $|a\rangle$. All contributions from the terms corresponding to $\rho^{(0)}_{bb}, \rho^{(0)}_{cc}, \rho^{(0)}_{dd}$ have been assumed zero due to their negligible initial population. Four transition dipole matrix elements $\langle n|\mu_p|m\rangle$ represent the four photon interactions involved in the CARS process, where the subindices $p$ refer to the polari-

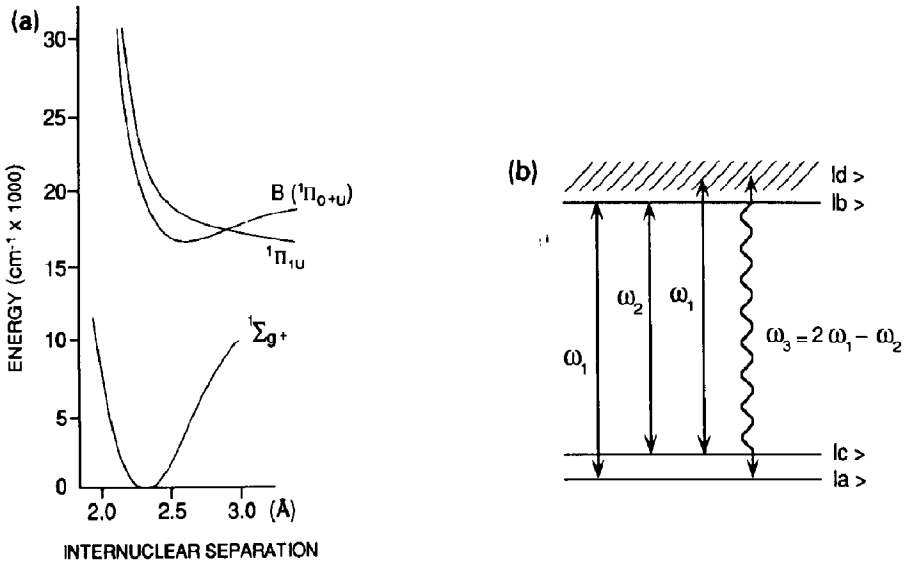


Fig. 4. (a) Potential energy curves of $Br_2$. The fixed pump laser frequency $\omega_1$ is in near resonance with $B\,^3\Pi^+_{u0}$–$X\,^1\Sigma^+_g$ transitions between particular rovibrational states $|b\rangle$ and $|a\rangle$ of which some are listed in table 1. (b) Energy level scheme for the resonance-enhanced CARS process in $Br_2$. The solid lines refer to bound states while the shaded area represents continuum states.

zation of the fields involved. $\omega_{ij}$ represents the transition frequency from state $|j\rangle$ to $|i\rangle$ in the medium. $\Gamma$ is the damping factor of the resonance involved.

Inspection of the resonance denominators in $\chi^{(3)}$ clarifies the assignment of the resonance CARS lines observed. As the frequency $\omega_1$ is fixed the pump wave selects several one-photon electronic resonances in $Br_2$ with small detuning $\delta\omega_{ba}=\omega_{ba}-\omega_1$. This absorption resonance may be considered as a "state selector" for particular ground states $|a\rangle$ that are probed in a CARS resonance. In table 1 the most important one-photon electronic resonances and relative initial populations of the various states are tabulated for all lines marked in fig. 1. The population distribution is calculated for thermal equilibrium at room temperature, and the percentages listed relate to the total number of molecules distributed over the three different isotopic species. Nuclear spin statistics ($I=3/2$ for both isotopes) was accounted for. The vibrational states involved in the one-photon resonance are given in table 1 in parentheses after the rotational assignment. Thus, P(20) (0, 25) denotes the one-photon resonance $J_a=20$, $v_a=0$, $X\,^1\Sigma_g^+ \rightarrow J_b=19$, $v_b=25$, $B\,^3\Pi_{u0}^+$.

A second resonance condition in $\chi^{(3)}$ is met when a Raman resonance between states $|c\rangle$ and $|a\rangle$ is obtained: $\omega_{ca}=\omega_1-\omega_2$. As $\omega_2$ is tuned this condition can always be fulfilled; the CARS resonance will appear at the specific frequency $\omega_2$ for which $\Delta\omega=\omega_1-\omega_2$ equals the Raman resonance $\omega_{ca}$. Due to the selectivity in the $\omega_1$ step only a few distinct lines are predicted in the spectra. Doublets are expected corresponding to either O and Q lines in the case of a P electronic resonance, or S and Q lines in the case of an R one-photon electronic resonance. These components of doublets probing the same ground-state population for state J are interconnected in the observed spectra (fig. 1).

The resonance in the third factor in the denominator of $\chi^{(3)}$ is a continuum resonance as in our experiments $\omega_{AS}>D_0$. The resonance condition $\omega_{AS}=\omega_{da}$ is always met, so no extra selectivity on rotational quantum number is added through this fac-

Table 1
Resonances, detunings and relative populations concerning the most prominent features in the $\Delta v=7$ spectrum of $Br_2$

| Molecule | $\omega_{ba}$ ($cm^{-1}$) | $\omega_{ba}-\omega_1$ ($cm^{-1}$) | Relative population (%) | $\omega_{ca}$ ($cm^{-1}$) |
|---|---|---|---|---|
| $^{79,79}Br_2$ | P(20) (0, 25) [a] | | | O(20) 2208.72 |
| | 18788.51 | +0.05 | 0.22 | Q(20) 2214.94 |
| | P(44) (0, 26) | | | O(44) 2197.51 |
| | 18788.53 | +0.07 | 0.23 | Q(44) 2211.36 |
| | R(22) (0, 25) | | | S(22) 2222.22 |
| | 18788.57 | +0.12 | 0.23 | Q(22) 2214.74 |
| | R(46) (0, 26) | | | S(46) 2226.06 |
| | 18788.19 | −0.27 | 0.23 | Q(46) 2210.94 |
| $^{79,81}Br_2$ | P(13) (0, 25) | | | O(13) 2198.22 |
| | 18788.87 | +0.41 | 0.43 | Q(13) 2202.15 |
| | P(81) (0, 30) | | | O(81) 2162.34 |
| | 18788.20 | −0.26 | 0.16 | Q(81) 2187.59 |
| | R(15) (0, 25) | | | S(15) 2207.21 |
| | 18788.94 | +0.48 | 0.48 | Q(15) 2202.02 |
| | R(58) (0, 27) | | | S(58) 2213.55 |
| | 18788.85 | +0.39 | 0.44 | Q(58) 2194.86 |
| $^{81,81}Br_2$ | P(39) (0, 26) | | | O(39) 2173.73 |
| | 18788.92 | +0.46 | 0.41 | Q(39) 2185.69 |
| | R(41) (0, 26) | | | S(41) 2198.53 |
| | 18788.76 | +0.30 | 0.40 | Q(41) 2185.33 |

[a] P(20) (0, 25) denotes the resonance $J=20$, $v=0$, $X\,^1\Sigma_{g^+} \rightarrow J=19$, $v=25$, $B\,^3\Pi_{u0}^+$.

tor, although enhancement of the FWM signal is obtained through this continuum resonance.

The actual identification of the observed CARS lines is based in first instance upon a determination of values for $\Delta\omega=\omega_1-\omega_2$. For this purpose first the fixed frequency $\omega_1$ of the pump laser is measured with an echelle grating and determined to be 18788.5(2) $cm^{-1}$. Secondly the CARS lines are calibrated in terms of the Stokes frequency by referencing them to the $I_2$-fluorescence spectrum [10]. Combination of pump and Stokes frequency then fixes the CARS resonances in $Br_2$ to within 0.2 $cm^{-1}$ on a scale of $\Delta\omega=\omega_1-\omega_2$. However, the molecular constants for the $X\,^1\Sigma_g^+$ state of $Br_2$ are accurately determined and term values of all rovibrational states are known within 0.001 $cm^{-1}$ [9]. So in principle positions of the CARS resonances are known to about the same accuracy on a scale of $\omega_1-\omega_2$. Using also polarization dependencies (see section 3.2) the individual rotational resonances in the CARS spectrum in $Br_2$ can be identified unambiguously. In fig. 1 an assignment based on these arguments is given for the most prominent features. The $J$ quantum number of the initial states probed, an assignment with O, Q and S according to the Raman branch and a subscript referring to the specific isotopic composition is given: I for $^{79,79}Br_2$, II for $^{79,81}Br_2$ and III for $^{81,81}Br_2$.

From the simultaneously recorded $I_2$-fluorescence spectrum the observed CARS resonances are accurately calibrated on the $\omega_2$ scale (within 0.015 $cm^{-1}$). As the position of the Raman resonances ($\omega_1-\omega_2$) are known (accuracy 0.001 $cm^{-1}$), from each individual line a value for the pump frequency $\omega_1$ may be derived. For the lines in the $\Delta v=7$ overtone of fig. 1 we find that all values fit within $18788.46\pm0.03$ $cm^{-1}$. The $2\sigma$ accurracy is 0.015 $cm^{-1}$. So the CARS spectra a posteriori result in an absolute frequency for the pump laser. Values for the various detunings $\delta\omega_{ba}$ follow from this determination of $\omega_1$. These detunings, listed in table 1 influence the intensities of the resonance CARS features (discussed below).

When comparing the spectral structure of the adjacent overtones $\Delta v=7$ and $\Delta v=8$ (shown in fig. 2) an apparent difference is found. A resonance at 2213.5 $cm^{-1}$ in the $\Delta v=7$ spectrum, identified as the $S_{II}(58)$ line, seems to have no counterpart in the $\Delta v=8$ overtone. However, calculation of energy positions shows that $S_{II}(58)$ coincides with the $Q_I(44)$ resonance at 2518.3 $cm^{-1}$ in the $\Delta v=8$ overtone.

### 3.2. Polarization effects

An additional tool in the identification of the lines in a resonance-enhanced CARS spectrum is the effect of polarization of the two lasers on intensity. In a previous study [11] it was shown that coherent four-photon linestrengths can be calculated for any polarization configuration. In a similar manner rotational linestrength factors $S_J$ were calculated for the particular resonance scheme of fig. 4. These rotational linestrengths depend on the value for the projection of the electronic angular momentum on the internuclear axis of the molecule, denoted by $\Omega$, in the appropriate Hund's case (c) coupling scheme. For the states $|a\rangle$, $|b\rangle$ and $|c\rangle$ these values are well defined for the particular resonance CARS wave mixing scheme: $\Omega_a=\Omega_b=\Omega_c=0$. In the summation over continuum states $|d\rangle$ both the dissociative continuum of the bound state $B\,^3\Pi_{u0}^+$, and the repulsive continuum of the $^1\Pi_{1u}$ state, with $\Omega_d=0$ and $\Omega_d=1$, respectively, may in principle contribute.

Potential energy curves for the $B\,^3\Pi_{u0}^+$ and $^1\Pi_{1u}$ states, including the energy range above the ($^2P_{3/2}$ and $^2P_{1/2}$) dissociation limit were constructed by Le Roy et al. [12]. From these curves extinction coefficients versus wavelength were calculated by Coxon et al. [5]. It follows that continuum absorption in the energy range up to 21000 $cm^{-1}$ is dominated by the $B\,^3\Pi_{u0}^+$ state. The contribution of $^1\Pi_{1u}$ state appears to be a factor 15 weaker in this range. In the energy range above 23000 $cm^{-1}$ the extinction coefficient related to $^1\Pi_{1u}$ is dominant; in the analysis of continuum resonance Raman spectra in $Br_2$ [13] it was indeed found that only the $^1\Pi_{1u}$ continuum contributes in the range 23000–30000 $cm^{-1}$. In the present discrete-continuum CARS experiment on the $\Delta v=7$ overtone the anti-Stokes wave is in resonance with a transition from the continuum near 21000 $cm^{-1}$, and we assume that the continuum enhancement is produced by the dissociative continuum of the $B\,^3\Pi_{u0}^+$ state. In the calculation of rotational linestrengths $S_J$ of O, Q and S lines therefore $\Omega_d=0$ is taken; results are listed in table 2. For the alternative case of enhancement by a continuum with $\Omega_d=1$ rotational linestrengths are also calculated and

Table 2
Rotational linestrength factors $S_J$ for $\Omega_d=0$, i.e. continuum enhancement by the $B\,^3\Pi_{u0}^+$ state

| | O lines | Q lines [a] | Q lines [b] | S lines |
|---|---|---|---|---|
| parallel | $\frac{2J(J-1)}{15(2J-1)}$ | $\frac{J(4J-1)}{15(2J-1)}$ | $\frac{-J(J+1)}{30(2J-1)}$ | $\frac{2(J+1)(J+2)}{15(2J+3)}$ |
| crossed | $\frac{-J(J-1)}{10(2J-1)}$ | $\frac{(J+1)(4J+5)}{15(2J+3)}$ | $\frac{-J(J+1)}{30(2J+3)}$ | $\frac{-(J+1)(J+2)}{10(2J+3)}$ |

[a] In the case of $J_b=J_a-1$. [b] In the case of $J_b=J_a+1$.

Table 3
Rotational linestrength factors $S_J$ for $\Omega_d=1$, i.e. continuum enhancement by the $^1\Pi_{1u}$ state

| | O lines | Q lines [a] | Q lines [b] | S lines |
|---|---|---|---|---|
| parallel | $\frac{J(J-1)}{15(2J-1)}$ | $\frac{-J(3J-2)}{15(2J-1)}$ | $\frac{-(J+1)(3J+5)}{15(2J+3)}$ | $\frac{(J+1)(J+2)}{15(2J+3)}$ |
| crossed | $\frac{-J(J-1)}{20(2J-1)}$ | $\frac{-J(J+1)}{60(2J-1)}$ | $\frac{-J(J+1)}{60(2J+3)}$ | $\frac{-(J+1)(J+2)}{20(2J+3)}$ |

[a] In the case of $J_b=J_a-1$. [b] In the case of $J_b=J_a+1$.

listed in table 3. In both cases calculations were performed for parallel and crossed linear polarizations of the incident laser beams. It should be noted that in the present case of discrete state resonance CARS two kinds of Q lines appear with a different linestrength: a Raman Q line involving either a P or an R line on the first photon resonance. The $M_J$ degeneracy of the initially populated levels is accounted for in the rotational linestrength factor. A general description of the theoretical procedures and a proof of the rotational linestrength expressions of tables 2 and 3 will be given in a forthcoming publication [14].

Within a particular overtone spectrum the dependence of relative line intensities on electronic transition moments and Franck–Condon factors of eq. (2) may be separated off [11]. The relative intensities are found to be proportional to

$$I_{\mathrm{CARS}} \propto \left( \frac{N\rho_{aa}^{(0)}}{2J_a+1} S_{J_a} \frac{1}{\delta\omega_{ba}\Gamma_{ca}\Gamma_{da}} \right)^2 , \qquad (3)$$

where the damping factor $\Gamma_{ba}$ of the Raman coherence ($<0.01$ cm$^{-1}$ at low pressures in the gas phase) is presumed much smaller than the detuning $\delta\omega_{ba}$. CARS resonances with small detuning $\delta\omega_{ba}$ (see table 1) on the first state selecting transition, such as the O–Q (20) and the O–Q (44) indeed tend to be intense. A usefull tool for line-assignment now is to consider the ratio of line intensities within a particular Q/O or Q/S doublet where the dependence on initial state populations $N\rho_{aa}^{(0)}$, Franck–Condon overlap integrals, electronic transition moments and detunings $\delta\omega_{ba}$ is eliminated. It is assumed that the damping parameters $\Gamma_{ca}$ and $\Gamma_{da}$ are equal for the different bound states $|c\rangle$ and the $|d\rangle$ continuum. In table 4 simple $J$-dependent expressions for the ratio of line intensities are given for the cases of parallel and crossed polarization; continuum enhancement by the $B\,^3\Pi_{u0}^+$ state (so $\Omega_d=0$) was assumed.

In the $\Delta v=7$ overtone spectrum of fig. 3 an intensity ratio between e.g. Q(44) and O(44) of 3.9 is estimated in the case of parallel polarization, while from table 4 a theoretical value of 4.4 follows. For

Table 4
Ratio of rotational line intensities within a particular doublet; continuum enhancement by the $B\,^3\Pi_{u0}^+$ state is assumed

| | Q/O | Q/S |
|---|---|---|
| parallel | $\left\lvert\frac{4J-1}{2(J-1)}\right\rvert^2$ | $\left\lvert\frac{4J+5}{2(J+2)}\right\rvert^2$ |
| crossed | $\left\lvert\frac{J+1}{3(J-1)}\right\rvert^2$ | $\left\lvert\frac{J}{3(J+2)}\right\rvert^2$ |

the crossed polarization spectrum we find values of 0.16 and 0.10 for observed and predicted ratios, respectively. As such these drastic dependencies of intensity ratios on polarization are a reliable check on the assignments of resonance CARS features in molecular bromine.

## 4. Final remarks

In the present Letter, the experimental observation in a two-color setup of strong resonance CARS features in natural $Br_2$ is reported. A particular four-wave-mixing process is identified that is threefold resonance enhanced: an electronic resonance of the pump laser with selected transitions in the $B\,^3\Pi_{u0}^+$–$X\,^1\Sigma_g^+$ system of $Br_2$, a vibrational or Raman resonance that is commonly encountered in CARS and a continuum resonance of the anti-Stokes wave with the dissociative range of the $B\,^3\Pi_{u0}^+$ state. Characteristic features in these type of discrete-continuum CARS processes are: appearance of intense overtone series and of doublets of singly resolved rotational lines as narrow as the bandwidth of the Stokes laser. In contrast to continuum CARS processes the pronounced and narrow features are produced by a single isotopic combination in $Br_2$.

The positions of the CARS lines could be explained on the basis of the accurately known spectroscopic constants of the B–X system of the different isotopes of $Br_2$. The assignment of all lines was checked by comparing relative intensities in both the parallel and the crossed polarization experiments, with a calculation of relative linestrengths.

In a previous study of resonance CARS in $I_2$, apart from the overtone sequence of vibrational coherences in the $X\,^1\Sigma_g^+$ electronic ground state, also two different excited-state resonance CARS processes could be identified with vibrational coherences in the $B\,^3\Pi_{u0}^+$-excited state. Despite thorough efforts these particular multiple resonance four-wave-mixing processes could not be observed in the iso-electronic system $Br_2$. Only the so-called ground state CARS overtone sequence was observed in $Br_2$.

At a resonance frequency $\Delta\omega = 3685\ \mathrm{cm}^{-1}$ strong CARS signals were observed, which we attributed to CARS in Br atoms. Br is produced in photodissociation of $Br_2$ by the pump laser at 532 nm. The spectra show the resolved hyperfine splitting of the $^2P_{1/2}$ level in Br, while the hyperfine structure of the $^2P_{3/2}$ level is not resolved and gives rise to asymmetric line profiles.

Finally a method was devised to accurately determine the wavelength of our fixed frequency narrow band pulsed pump laser ($\omega_1$) by means of resonance CARS in $Br_2$. As the resonances all occur at $\omega_1 - \omega_2 = \omega_{\mathrm{Raman}}$, and distinct lines are observed in the present CARS experiment, the calibration accuracy of the tunable laser ($\omega_2$) limits the accuracy in $\omega_1$ in this experiment to $0.015\ \mathrm{cm}^{-1}$.

## References

[1] W. Holzer, W.F. Murphy and H.J. Bernstein, J. Chem. Phys. 52 (1970) 399.
[2] P.F. Williams and D.L. Rousseau, Phys. Rev. Letters 30 (1973) 951.
[3] D.L. Rousseau and P.F. Williams, J. Chem. Phys. 64 (1976) 3519.
[4] W. Kiefer and P. Baierl, J. Raman Spectry. 3 (1975) 353.
[5] J.A. Coxon, N. Gramari and M. Jacon, J. Raman Spectry. 8 (1979) 63.
[6] P. Baierl and W. Kiefer, J. Raman Spectry. 10 (1981) 197.
[7] A. Beckmann, H. Fietz, P. Baierl and W. Kiefer, Chem. Phys. Letters 86 (1982) 140.
[8] I. Aben, W. Ubachs, P. Levelt, G. v.d. Zwan and W. Hogervorst, Phys. Rev. A 44 (1991) 5881.
[9] S. Gerstenkorn and P. Luc, J. Phys. (Paris) 50 (1989) 1417.
[10] S. Gerstenkorn and P. Luc, Atlas du spectre d'absorption de la molecule d'iode, (Editions du CNRS, Paris, 1977).
[11] I. Aben, W. Ubachs, G. v.d. Zwan and W. Hogervorst, Mol. Phys., accepted for publication.
[12] R.J. Le Roy, R.G. Macdonald and G. Burns, J. Chem. Phys. 65 (1976) 1485.
[13] J. Strempel and W. Kiefer, J. Raman Spectry. 22 (1991) 583.
[14] I. Aben, W. Ubachs, G. v.d. Zwan and W. Hogervorst, in preparation.